Forensic Science International 347 (2023) 111690

Contents lists available at ScienceDirect

Forensic Science International

journal homepage: www.elsevier.com/locate/forsciint

Differentiating present-day from ancient bones by vibrational spectroscopy upon acetic acid treatment

A.L.C. Brandão [a], L.A.E. Batista de Carvalho [a,*], D. Gonçalves [b,c,d], G. Piga [b,e], E. Cunha [b,f,g], M.P.M. Marques [a,f]

[a] University of Coimbra, Molecular Physical-Chemistry R&D Unit, Department of Chemistry, 3004-535 Coimbra, Portugal
[b] University of Coimbra, Laboratory of Forensic Anthropology, Centre for Functional Ecology, 3000-456 Coimbra, Portugal
[c] University of Coimbra, Research Centre for Anthropology and Health (CIAS), 3000-456 Coimbra, Portugal
[d] Archaeosciences Laboratory, Directorate General Cultural Heritage (LARC/CIBIO/InBIO), 1349-021 Lisbon, Portugal
[e] University of Sassari, DISSUF - Department of History, Human Sciences and Education, Italy
[f] University of Coimbra, Department of Life Sciences, 3000-456 Coimbra, Portugal
[g] Institute of Legal Medicine and Forensic Sciences, 1169-201 Lisbon, Portugal

ARTICLE INFO

Article history:
Received 16 June 2022
Received in revised form 7 December 2022
Accepted 11 April 2023
Available online 14 April 2023

Keywords:
FTIR-ATR spectroscopy
Raman spectroscopy
Post-mortem interval
Controlled burning
Cremation
Carbonate content

ABSTRACT

Acetic acid treatment for an accurate differentiation between ancient and recent human bones was assessed using Raman and FTIR-ATR spectroscopies. Each set of skeletal samples was analysed by these techniques, prior and after chemical washing, in order to determine the variations in bone´s chemical composition and crystallinity. Bone samples were collected from several independent sources: recent bones burned under controlled experimental conditions or cremated, and archaeological (XVII century and Iron Age). The effect of acetic acid, expected to impact mostly on carbonates, was clearly evidenced in the spectra of all samples, particularly in FTIR-ATR, mainly through the bands typical of A- and B-carbonates. Furthermore, as seen for crematoria and archaeological samples, acetic acid was found to remove contaminants such as calcium hydroxide. Overall, acetic acid treatment can be an effective method for removing carbonates (exogenous but possibly also endogenous) and external contaminants from bone. However, these effects are dependent on the skeletal conditions (*e.g. post-mortem* interval and burning settings). In addition, this chemical washing was shown to be insufficient for an unequivocal discrimination between recent and archaeological skeletal remains. Based on the measured IR indexes, only cremated bones could be clearly distinguished.

1. Introduction

The antiquity of human skeletal remains can be difficult to establish, this being paramount to determine what kind of investigation is appropriate – archaeological or forensic. The direct estimation of the post-mortem interval (PMI) of bones and teeth is at times challenging, despite several methods being available with varied efficacies, such as radiocarbon dating [1], luminol [2,3] or determination of the citrate content of bone [4,5]. Often, these methods are not applicable, and experts are required to rely on PMI estimations obtained indirectly, *i.e.,* based on other than skeletal remains (*e.g.,* entomology; botany, dateable objects). The challenge is even greater when skeletal remains have been exposed to heat since such methods may not be applicable or may be expensive (as in the case of radiocarbon dating). Therefore, forensic anthropology lacks a rapid and cheap method able to circumvent the heat-elicited changes in burned skeletal remains and to discriminate between present-day and ancient bones.

Fourier transform infrared (FTIR) spectroscopy has been a technique of choice for the study of bone tissue, even upon extensive burning, since it enables a molecular analysis with high accuracy and sensitivity, providing reliable information on the diagenetic and/or heat-induced alterations at both the chemical and structural levels [6–28]. In particular, FTIR in attenuated total reflectance (ATR) mode, avoiding any type of sample preparation and requiring minimal amounts of sample, has become the most commonly used, rapid and non-invasive spectroscopic tool for the analysis of skeletal remains in both forensic [9,11,20,21,29,30] and archaeological settings [10,16,19,24,31,32]. Spectroscopic relationships such as the crystallinity index (CI), the carbonate/phosphate and the hydroxyl/phosphate ratios, are reported to be highly valuable parameters for the analysis of burned bones [10,12,17,22,24,26,29,33]. Some preliminary research about the potential of infrared spectroscopy for *post-*

* Corresponding author.
E-mail address: labc@ci.uc.pt (L.A.E. Batista de Carvalho).

https://doi.org/10.1016/j.forsciint.2023.111690

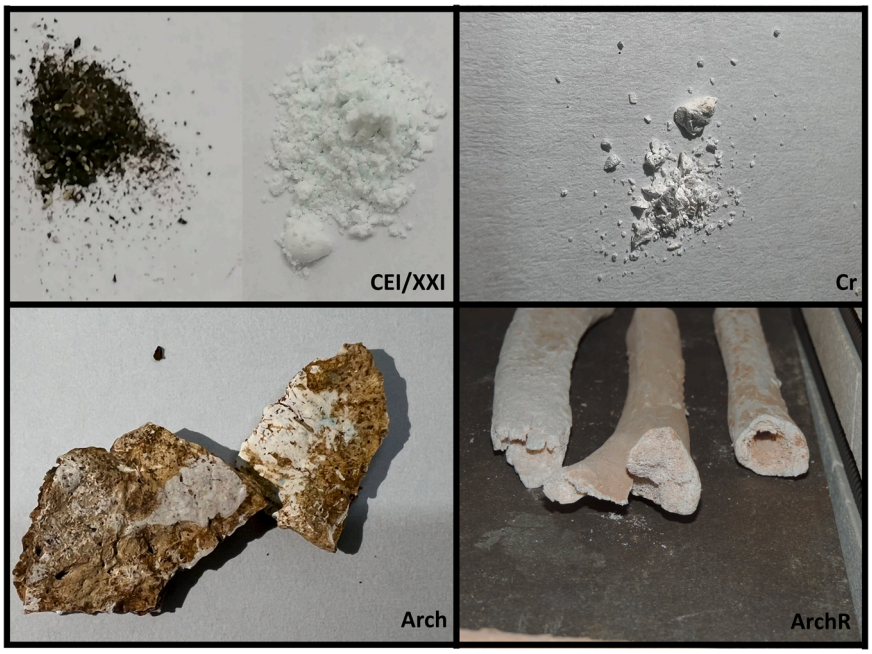

Fig. 1. Human skeletal samples analysed in the present study: CEI/XXI – a collection of present-day identified skeletons (University of Coimbra, Portugal); Cr – present-day cremated bones (Trieste, Italy); Arch – ancient archaeological bones (El Inchidero necropolis, Spain); ArchR – recent archaeological bones (Porto, Portugal).

mortem interval estimations has been carried out recently [34–38] but further investigation on the potential effect of diagenesis on the results is still needed. Also, none of these attempts focused specifically on burned bones.

Bone is a biphasic heterogeneous material that comprises organic constituents (*ca.* 20 wt%, collagen type I and lipids) interwoven with in plate-like mineral nanocrystals of non-stoichiometric hydroxyapatite ($Ca_{10}(PO_4)_6OH_x$, HAp, *ca.* 70 wt%), the hydroxyl and phosphate groups being partly substituted by carbonates (2–8%) – respectively A- and B-type, the latter being the predominant [26,39–42]. In addition to collagen interactions with this mineral phase of bone, carbonate concentration and substitution type controls the morphology, crystallite nanoscale size, solubility and mechanical properties of bioapatite [42,43], which determine bone´s physiological function.

Upon diagenesis (*post-burial* processes leading to physical and chemical alterations [11]) or after exposure to heat, bone experiences changes in chemical composition (lipid, protein and carbonate contents), structure and crystallinity, which are accompanied by macroscopic variations (in colour, dimensions and mass) [6,9,12,18,21,22,27,44–46]. Apart from the temperature and duration of the burning process, other factors can determine the heat impact on bones such as the bone morphology, the heating conditions regarding oxygen availability and the type of surrounding medium (*e.g.* chemical composition of the soil and groundwater, presence of metal ions or pollutants) which may lead to bone contamination through adsorption or inclusion of exogenous trace elements (*e.g.* Mg^{2+}, Sr^{2+}, Hg^{2+}, Cl^-, F^-, HPO_4^{2-} or labile CO_3^{2-}) that can exchange with endogenous chemical constituents [21,26,32,37,39,46–51]. These early diagenetic phenomena may overrule the *in vivo* chemical and structural profiles of the bone, and therefore confound further analysis and hinder the retrieval of reliable information. However, they may also provide a platform to attempt a general PMI estimation.

Treatment with acetic acid has been applied by several authors to remove soluble mineral contaminants from bone, namely diagenetic carbonates (exogenous carbonates such as calcite ($CaCO_3$)) [24,37,42,47–57]. This procedure aims at recovering the original biogenic bone composition and structure, thus allowing to obtain accurate information (*e.g.,* through radiocarbon dating or FTIR). Snoeck et al. applied acetic acid treatment to human bones [24] and verified that this procedure was able to remove contaminations as well as carbonates. Exogenous carbonates can be generated under different conditions, namely involving burial environments. These authors hypothesized that a treatment with acetic acid would have different effects on archaeological *vs.* recent bones. Since archaeological bones remain for longer times in burial environments, they should acquire more exogenous carbonates, which would lead to larger losses upon acetic acid washing as compared to recent bones. Nevertheless, their experimental results did not confirm this hypothesis since recent bones showed the greatest decrease in carbonates.

The current work applied FTIR-ATR to assess the impact of acetic acid treatment on bone´s chemical and structural profiles – either solely on exogenous carbonates or also on endogenous carbonates. Human skeletal samples from different sources and chronologies were probed: (i) present-day skeletal remains subjected to controlled aerobic burning between 450 and 1000 °C (electric furnace); (ii) cremated bones from a gas-fuelled present-day commercial crematorium; (iii) recent archaeological inhumed remains subjected to controlled aerobic burning (electric furnace); and (iv) ancient archaeological cremated remains from an Iron Age necropolis. The objective was to determine if an accurate discrimination between present-day and archaeological burned bones could be achieved based on the corresponding infrared profiles obtained both prior and after acetic acid treatment. If so, this procedure would constitute a rapid, inexpensive, and minimally destructive approach to identify human skeletal remains with forensic relevance, which would be an added value for routine cases of forensic anthropology.

2. Materials and methods

2.1. Materials

Samples of fresh porcine bone (obtained at a local market), burned at 450 °C, 500 °C, 700 °C, 900 °C and 1000 °C, were used to optimise the experimental protocol of acetic acid treatment.

Four sets of human skeletal samples were analysed in this study, two comprising present-day bones and two containing archaeological skeletal remains (Fig. 1, Table S1/Supplementary Information):

(I) *CEI/XXI* – specimens of present-day femur (n = 8), radius (n = 8), tibia (n = 8), ulna (n = 8), humerus (n = 8), talus (n = 4), pelvis (n = 3), coxae (n = 1), clavicle (n = 6), fibula (n = 8), metacarpals (n = 18) and metatarsals (n = 20), from four human skeletons formerly from the cemetery of Capuchos (Santarém, Portugal) and now part of the 21st Century Identified Skeletal Collection housed at the Laboratory of Forensic Anthropology of the University of Coimbra (Portugal) [58]. Skeletons were from individuals of known sex and age at death, which occurred between 1982 and 2012, being inhumed for ten years on average (three years is the minimum period of inhumation time before exhumation according to Portuguese legislation, Decreto-Lei 411/98). Authorization for research on this collection was granted by the Ethics Committee of the Faculty of Medicine of the University of Coimbra (reference number: CE_026.2016).

(II) *Cr* – 24 specimens of present-day cremated bones (powdered samples) subjected to temperatures from 850 to 1150 °C. These samples, consisting of small femoral midshaft fragments were obtained from the collection of small samples of historical or controlled cremated bones - including anonymised human commercial cremation - belonging to Research Unit of Paleoradiology and Allied Sciences, Julian-Isontine Universitary Integrated Health Enterprise (ASUGI), Trieste (Italy).

(III) *ArchR* – 15 specimens of recent archaeological bones from the cemetery associated with the former *Hospital Real de Santo António* (Porto, Portugal), belonging to skeletons from the XVII to early XX centuries. These were merely inhumed bones which, for research purposes, were later subjected to experimental burning at 900 °C [59].

(IV) *Arch* – 18 specimens of ancient archaeological cremated bones from the Iron Age necropolis of El Inchidero [Aguilar de Montuenga (Soria), Spain].

The highly crystalline SRM 2910b calcium hydroxyapatite (HAp, $Ca_{10}(PO_4)_6(OH)_2$, Ca/P = 1.67) from NIST (Gaithersburg/MA, USA) [NIST] was used as a reference material (crystallinity index=7.91, as compared to 3.79 for commercial HAp).

2.2. Experimental burning

The samples from sets CEI/XXI and ArchR were subjected to controlled experimental burning. These bones were dry (*i.e.,* completely devoid of soft tissue and marrow) and were neither dehydrated nor degreased. Bone sections (*ca.* 2 cm in length) were cut with a DREMEL® mini-saw electric tool (model 395).

The burning process was carried out in an electric muffle furnace (BARRACHA model K-3, three-phased, 14 A manufactured by Barracha Lda., Leiria, Portugal, 1994) coupled to an automatic programmer allowing programmed start-up and automatic heating speed variation. A type K thermocouple (negative/nickel-aluminium, positive/nickel-chrome) was used to measure the temperature inside the furnace (according to norm IEC 60584–2) which was displayed on a digital temperature indicator. The following maximum temperatures and durations were applied (for a heating rate of *ca.* 6–10 °C/min): 450 °C (120 min), 700 °C (120 min), 800 °C (180 min) and 900 °C (180 min). These burn durations reflect the time required to attain each maximum temperature, after which the furnace was switched off. Before removal from the furnace, the samples were left to cool to room temperature.

2.3. Treatment with acetic acid

Before the experiments on human samples, the experimental procedure for acetic acid treatment was optimized using faunal bone (porcine femur): in independent experiments, small scrapes from fresh (deflected) bones were immersed in three different acetic acid aqueous solutions – 0.1, 0.5 or 1.0 M – in a 0.04 mg/mL proportion, following previous reports [50,57], and left with stirring (at room temperature) for different periods – 2, 3, 4, 6, 8 or 15 h. After each time, the samples were repeatedly washed with deionized water, filtered under vacuum or centrifuged (for the fine powdered samples) and dried at 70 °C in a muffle furnace. This optimization process provided the best experimental conditions (assessed by infrared spectroscopy), which were subsequently applied to the human bone samples under study.

After burning at the defined temperatures (450, 700, 900 and 1000 °C), each human bone fragment from sets CEI/XXI, ArchR and Arch was scraped with a scalpel to very small splinters and was subjected to acetic acid treatment. The cremated bones (Cr) were treated with acetic acid as received. Each sample was weighed before and after treatment, in triplicate, the average value having been considered (to determine the weight loss upon acid treatment).

2.4. FTIR-ATR spectroscopy

FTIR data was recorded, in attenuated total reflectance (ATR) mode, in the mid-IR interval (400–4000 cm^{-1}), in a Bruker Optics Vertex 70 FTIR spectrometer purged by CO_2-free dry air and equipped with a Bruker Platinum ATR single reflection diamond accessory. A liquid nitrogen-cooled wideband mercury cadmium telluride (MCT) detector and a Ge on KBr substrate beamsplitter were used.

128 scans were averaged for each spectrum (and background), at 2 cm^{-1} resolution, applying the 3-term Blackman–Harris apodization function, yielding a wavenumber accuracy above 1 cm^{-1}. The Bruker OPUS – Spectroscopy Software (8.1 version) was used to correct the spectra regarding the wavelength dependence of the penetration depth of the electric field in ATR, using a mean refractive index of 1.25. The spectra were normalized to the ($\nu_3(PO_4^{3-})$) band at 1030 cm^{-1}.

Peak heights (rather than areas) were considered for calculating the following spectroscopic ratios: CI ($\nu_4(PO_4^{3-})/I_{565} = (I_{595} + I_{603})/I_{565}$), C/P ($\nu_3(CO_3^{2-})_B/\nu_3(PO_4^{2-}) = I_{1415}/I_{1030}$), BPI ($((\nu_3(CO_3^{2-})_B/\nu_4(PO_4^{3-}) = I_{1415}/I_{603})$, API ($((\nu_3(CO_3^{2-})_A/\nu_4(PO_4^{3-}) = I_{1540}/I_{603})$, C/C ($\nu_3(CO_3^{2-})_{A+B}/\nu_3(CO_3^{2-})_B = I_{1450}/I_{1415}$) and OH/P ($OH_{lib}/\nu_4(PO_4^{3-}) = I_{630}/I_{603}$) (Table 1, Fig. 2).

2.5. Raman spectroscopy

Raman spectra were obtained from a WITec confocal Raman microscope system alpha300 R, coupled to an ultra-high throughput spectrometer (UHTS 300 VIS-NIR, f/4, 300 mm focal length, 600 groves *per* millimetre blazed for 500 nm). The detection system was 1650 × 200 pixels thermoelectrically cooled (−55 °C at room temperature) charge-coupled device camera, front-illuminated with NIR/VIS antireflection coating, with a spectral resolution < 0.8 cm^{-1}/pixel. The excitation radiation was a WITec 532 nm laser, yielding *ca.* 20 mW at the sample position. A 10x objective (Zeiss Epiplan, NA 0.23, WD 16.1 mm) was used. 10 accumulations were collected *per* sample, with 30 s exposure time. The spectra were normalized to the $\nu_1(PO_4^{3-})$ band at 960 cm^{-1}.

3. Results and discussion

3.1. Procedure optimization

Porcine bone fragments burned at 300 °C, 500 °C, 700 °C, 900 °C, 1000 °C, as well as an unburned fragment (control), were used for

Table 1
Spectroscopic ratios used in the current analysis, based on infrared and Raman bands.

Method	Index		Spectroscopic ratios	Reference
FTIR	CI	Degree of crystallinity	$\frac{(Abs(603cm^{-1})+Abs(565cm^{-1})}{Abs(590cm^{-1})}$	[12,60–63]
	BPI	Carbonate B	$\frac{Abs(1415cm^{-1})}{Abs(603cm^{-1})}$	[12,24,45,60,62,64]
	API	Carbonate A	$\frac{Abs(1540cm^{-1})}{Abs(603cm^{-1})}$	[45,60,62,64]
	C/C	Carbonate (A+B) to carbonate B	$\frac{Abs(1450cm^{-1})}{Abs(1415cm^{-1})}$	[7,12,24,45,60,62]
	C/P	Carbonate B to phosphate	$\frac{Abs(1415cm^{-1})}{Abs(1035cm^{-1})}$	[6,7,48,61,62,65,66]
	OH/P	Amount of OH^- groups	$\frac{Abs(630cm^{-1})}{Abs(603cm^{-1})}$	[12,22,24,45,60]
			$\frac{Abs(3572cm^{-1})}{Abs(603cm^{-1})}$	[60]
			$\frac{Abs(340cm^{-1})}{Abs(603cm^{-1})}$	[60]
	CN/P	Cyanamide to phosphate	$\frac{Abs(2010cm^{-1})}{Abs(1035cm^{-1})}$	[11,67]
	Am/P	collagen to phosphate	$\frac{Abs(1650cm^{-1})}{Abs(1035cm^{-1})}$	[11,65]
	CO/CO_3	protein to carbonate	$\frac{Abs(1650cm^{-1})}{Abs(1415cm^{-1})}$	[11]
	CO_3/P	Carbonate to phosphate	$\frac{Abs(900cm^{-1})}{Abs(1035cm^{-1})}$	[11]
Raman	Amount of Phosphate		$A(429cm^{-1})/A(1215cm^{-1})$	[60,68]
			$A(960cm^{-1})/A(1616cm^{-1})$	[11,69]
	Mineral matrix/crystallinity		$1/FWHM(960cm^{-1})$	[60,68]
	Carbonate to phosphate		$A(1070cm^{-1})/A(960cm^{-1})$	[60,70]
			$A(1070cm^{-1})/A(422cm^{-1})$	[60]
	Amount of OH^- groups		$A(3572cm^{-1})/A(422cm^{-1})$	[60]
	Collagen preservation		$I(960cm^{-1})/I(1636cm^{-1})$	[11,24]

Abs – Absorbance; A – Area; I – Intensity; FWHM – Full Width at Half Maximum

optimizing the experimental conditions of acetic acid treatment. Three bone fragments were treated with acetic acid at three different concentrations – 1.0, 0.5, and 0.1 M – for 2 and 15 h.

Treatment with acetic acid at 0.1 M resulted in a 50% mass loss, while the higher concentrations caused losses of about 60% (Table 2). Additionally, the largest decrease of the BPI (B-type carbonates) and C/P indices were achieved with 0.1 and 0.5 M acetic acid. Thus, the best conditions for carbonate removal were determined to be 0.1 M non-buffered acetic acid, since it induced the smallest mass loss coupled to the greatest decrease in BPI and C/P.

Following the establishment of the optimal acetic acid concentration, the most appropriate treatment time was determined. As

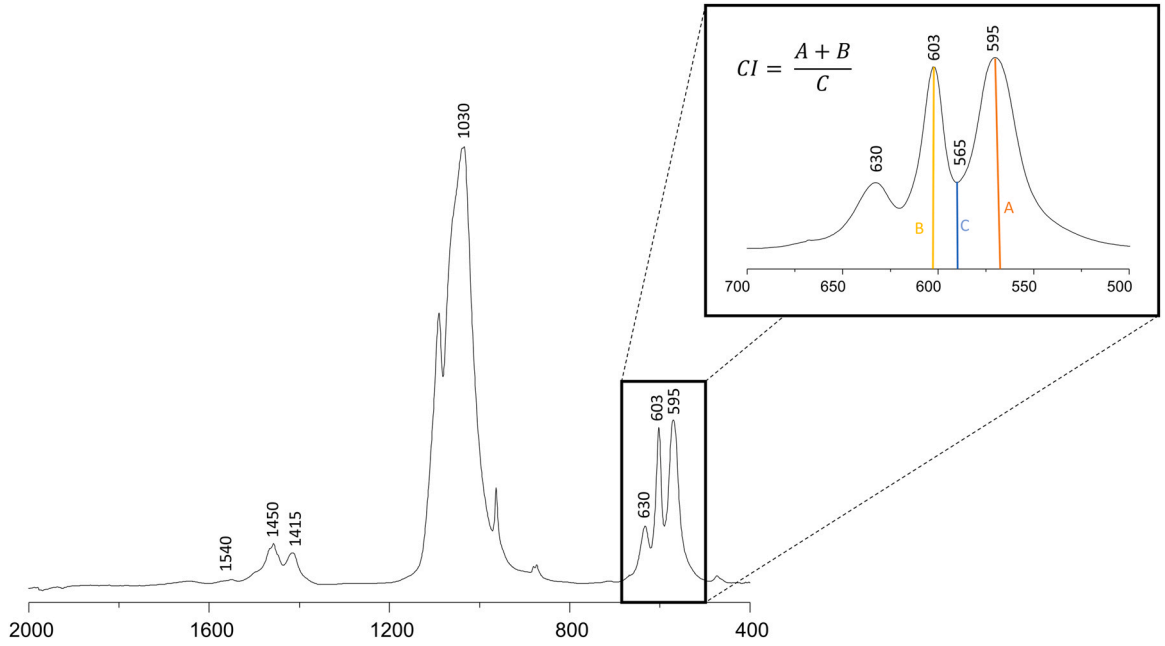

Fig. 2. Graphical representation of the infrared bands used for the calculation of the spectroscopic ratios CI, C/P, BPI, API, C/C, OH/P.

Table 2
Average mass, CI, C/P, API and BPI variations of the samples treated with acetic acid 1.0, 0.5, and 0.1 M.

concentration (M)	Time (h)	Mass Losses (%)	CI (%)	C/P (%)	API (%)	BPI (%)
1.0	2	59.7	19.9	-41.7	20.9	-40.6
	15	76.4	10.9	-22.4	53.2	-23.3
0.5	2	66.8	21.9	-33.4	-	-39.5
	15	77.6	19.7	-49.0	-	-41.9
0.1	2	52.9	18.0	-51.8	9.2	-51.0
	15	47.3	24.3	-51.2	23.5	-48.6

a result, acetic acid treatment (0.1 M) was applied to porcine samples burned at 300 and 1000 °C for 2, 3, 4, 6, 8 and 15 h. The most suitable treatment time was 4 h. For this treatment time, a pH change occurred – from 2.95 immediately after addition of acetic acid up to *ca.* 4.5 at the end of the acid washing procedure – evidencing carbonate removal from the bone matrix to the solution (with concomitant formation of HCO_3^- species, followed by CO_2 release).

Hence, the optimized conditions for acetic acid treatment were: 4-hours treatment with non-buffered 0.1 M-acetic acid. The samples showed mass losses lower 50%, the CI has increased by 12.8% and exogenous carbonate losses were more pronounced than in other periods (Fig. 3).

These results are in line with previous studies that revealed sample dissolution and recrystallization issues when using higher acetic acid concentrations (*e.g.,* 1.0 M), and a saturation effect for treatment times above 4 h [49,50,52].

3.2. Spectral profile

While the acid had a significant impact on bone unburned and lightly burned (at *ca.* 300 °C), it did not affect the samples burned at high temperatures (900 or 1000 °C) since these contain only trace amounts of carbonates (which were previously reported to disappear at these high temperatures under oxidative heating conditions [21]). The effectiveness of this chemical treatment for removing endogenous carbonates and exogenous trace elements depends on bone´s diagenetic state and processes it has been subjected to – such as burning (*e.g.,* cremation), inhumation and type of burial [37]. Actually, bones from diverse sources have distinct physical and chemical characteristics, which are expected to affect their response to acid treatment.

The effectiveness of acetic acid treatment was found to be the same for all bones, but the amount of carbonates acquired during either diagenesis or combustion greatly influences their physical and chemical characteristics. Each sample was therefore expected to behave differently when treated with acetic acid [37].

The FTIR-ATR data indicated that the acetic acid treatment predominantly affected the degree of carbonation of bone´s inorganic matrix (Fig. 4). The $\nu_3(PO_4^{3-})$ (at 1035 cm^{-1}) and $\nu_4(PO_4^{3-})$ (at 563 and 603 cm^{-1}) were the most appropriate signals for assessing the bone´s phosphate composition, since $\nu_2(PO_4^{3-})$ (at *ca.* 460 cm^{-1}) had a very low infrared intensity and $\nu_1(PO_4^{3-})$ (at 960 cm^{-1}) may be overruled by the very intense $\nu_3(PO_4^{3-})$ signal (mainly in low crystallinity samples). In turn, the $\nu_3(CO_3^{2-})_{A+B}$, $\nu_3(CO_3^{2-})_A$ and $\nu_3(CO_3^{2-})_B$ modes were used for assessing the carbonate content in the samples.

A clear reduction of the carbonate content was observed for all types of samples due to acetic acid washing, except for CEI/XXI-450

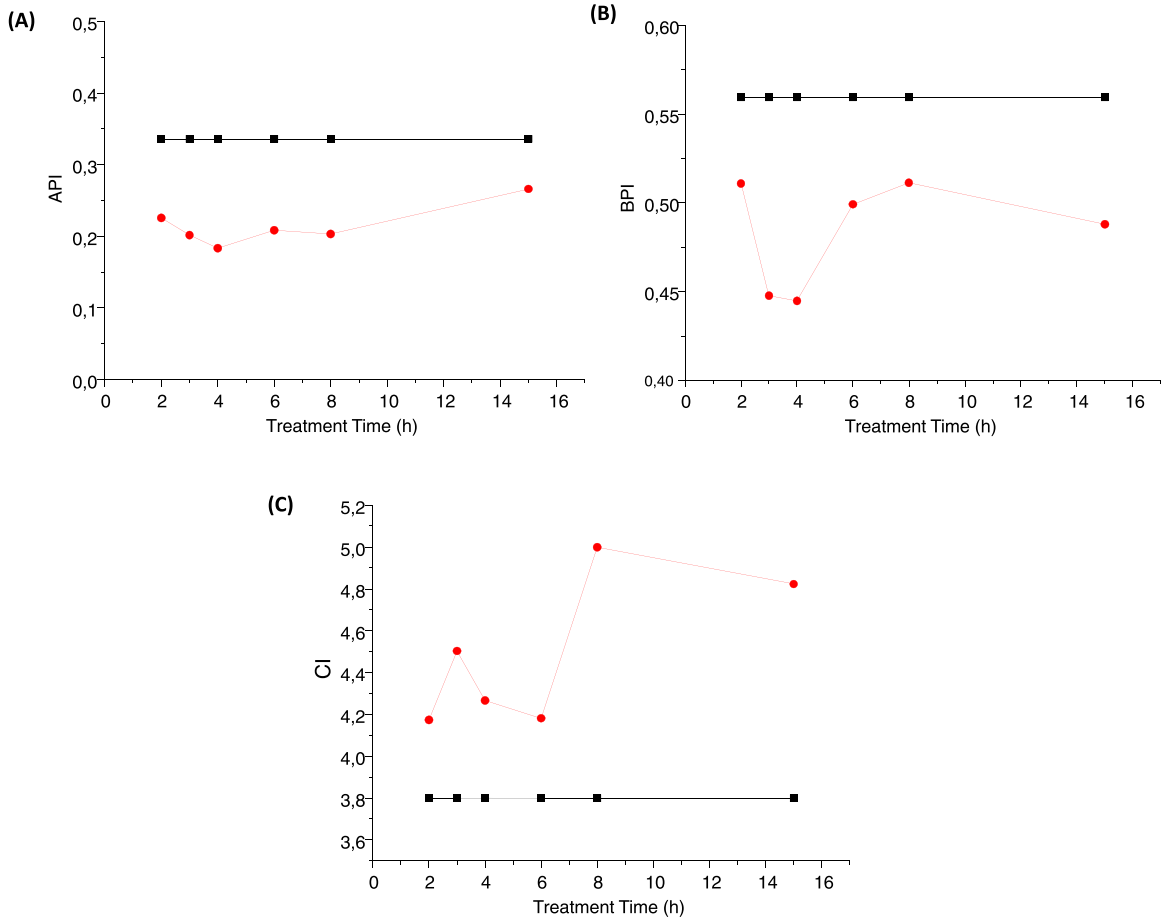

Fig. 3. Average values of API (A), BPI (B) and CI (C) for samples from porcine bones, before (black) and after (red) acetic acid treatment for different periods of time.

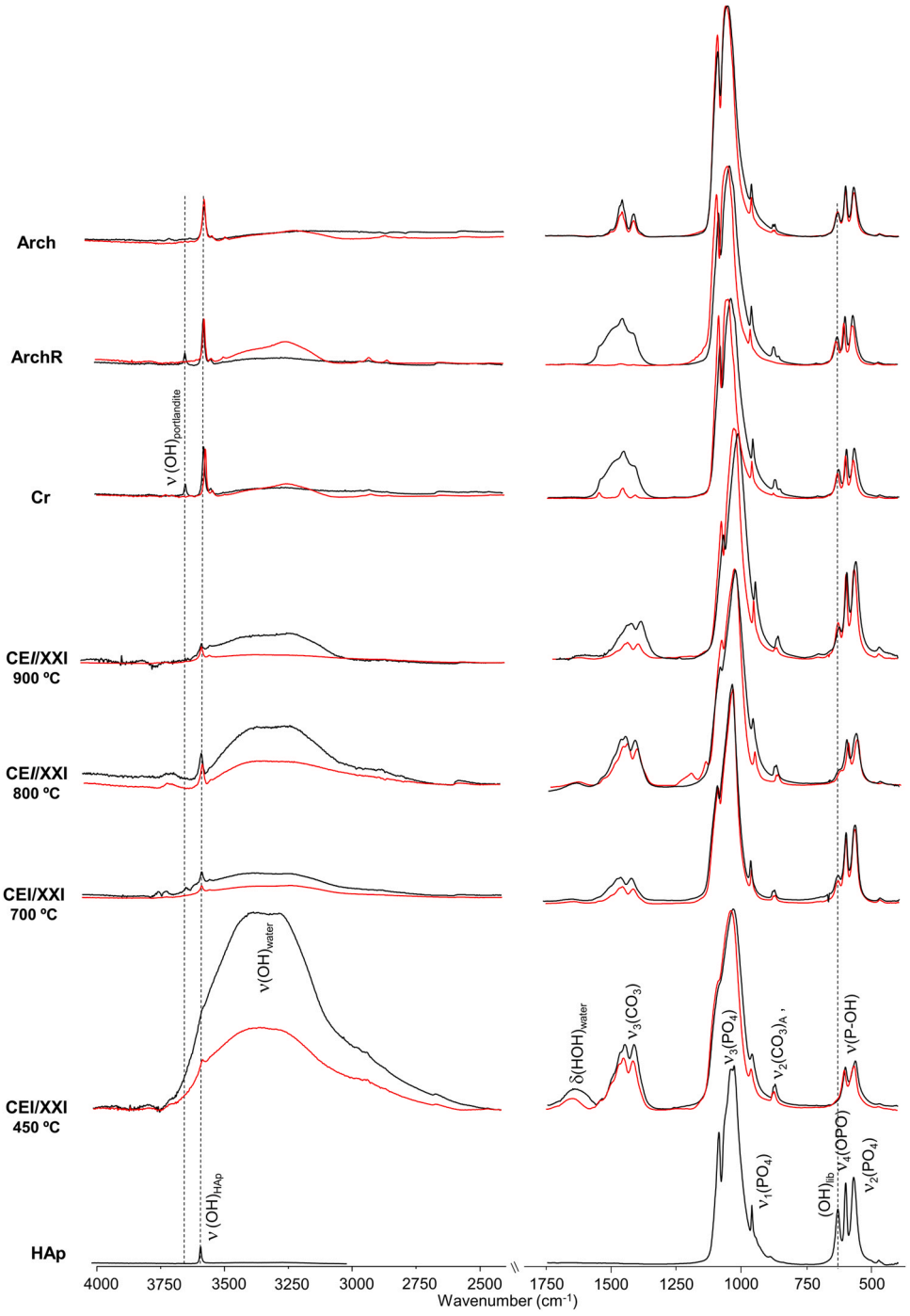

Fig. 4. FTIR-ATR spectra (400 – 4000 cm^{-1}) of selected human skeletal samples from CIE/XXI-450 °C, Cr, ArchR and Arch samples, before (black) and after (red) acetic acid treatment. The spectrum of reference hydroxyapatite (HAp, SRM 2910b) is also shown, for comparison purposes.

°C and Cr, for which a C/P increase was observed. It is known that the recently burned bones have smaller and more reactive crystals which, due to the absence of organic matter, begin to grow spontaneously [71]. This increase in the average crystal size is due to the removal of smaller crystals or the spontaneous growth of the crystal (or both). Over time, larger and less reactive (more stable) crystals begin to form that are not affected by acetic acid. Thus, it was expected that recently burned bones suffered a more pronounced effect by treating with acetic acid than the ancient burned bone samples, as observed by Snoeck et al. [24]. However, we found largest reductions of carbonates in recent archaeological bones which did not present post-treatment carbonate peaks. In contrast, the smallest carbonates reduction was observed in the CEI/XXI samples burnt at 450 °C. It should be noted that all types of samples presented variable reactions to the acetic acid treatment so no clear trend was observed. Although most *El Inchidero* samples experienced small carbonates reductions after the treatment, as previously reported by Snoeck et al. (2014) for archaeological samples, such specific behaviour was also observed for some present-day samples.

In addition, the Cr and Arch samples displayed a distinctive peak from portlandite ($Ca(OH_2)$) at 3643 cm^{-1}(apart from the characteristic ν(OH) from hydroxyapatite at 3571 cm^{-1}), which disappeared upon acid treatment. This may be due to contamination from the soil, for the archaeological samples, or even from CaO that might

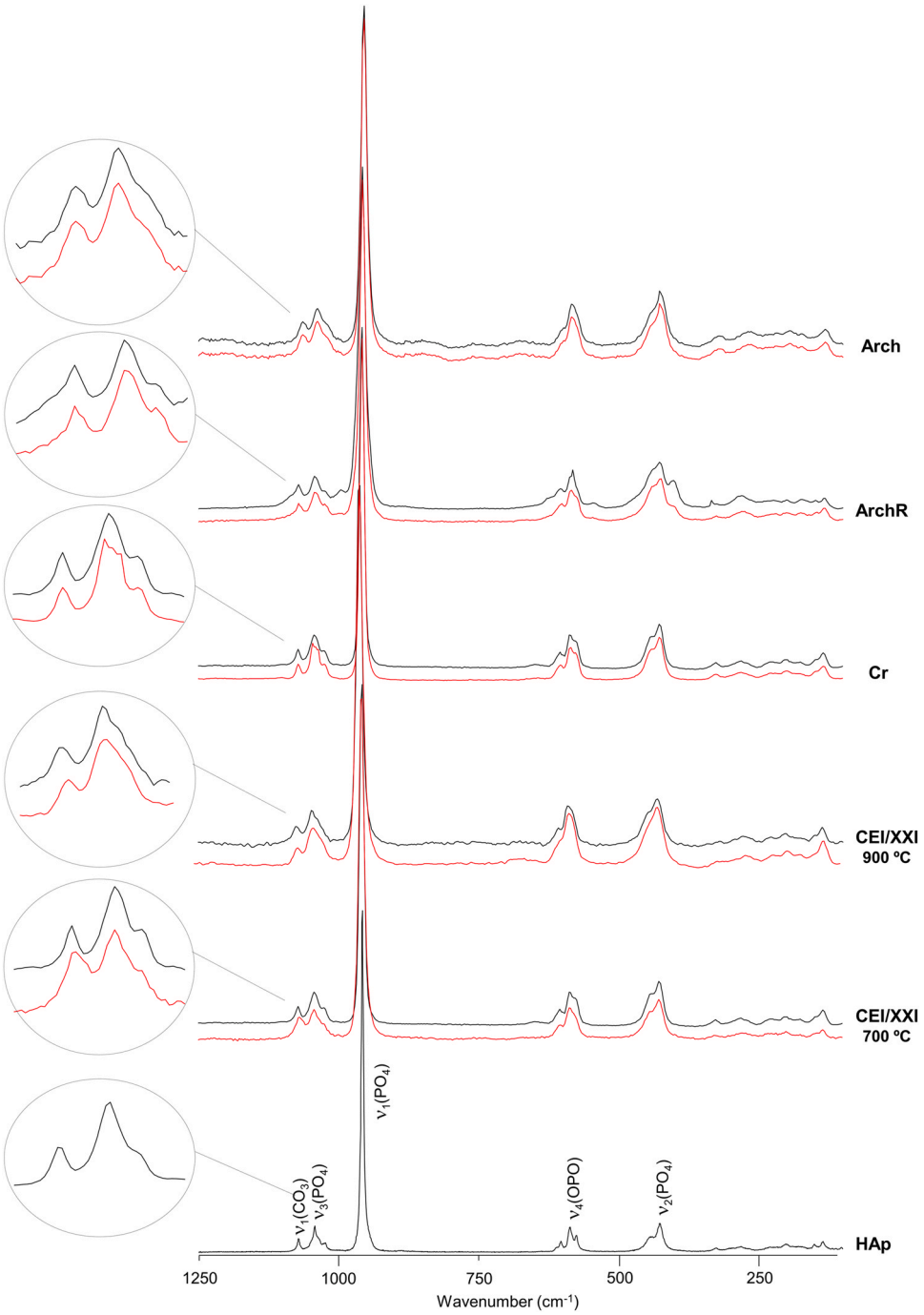

Fig. 5. Raman spectra (100 – 1250 cm^{-1}) of human skeletal samples from the CEI/XXI-700 and CEI/XXI-900 °C, Cr, ArchR and Arch sets of samples before (black) and after (red) acetic acid treatment. The spectrum of reference hydroxyapatite (HAp, SRM 2910b) is also shown, for comparison purposes.

have been added to the corpses. It should be emphasized that no portlandite was detected for the ArchR or CEI/XXI sets of samples, which are inhumed skeletal remains inside a coffin. Also, all samples, except samples at 450 °C, have a stretching OH at 3544 cm^{-1}.

Regarding the present-day skeletal samples (CEI/XXI) and the ancient archaeological bones (ArchR), distinctive vibrational bands from water were detected, more noticeable before acetic acid treatment, at 1620–1630 cm^{-1} (δ(HOH)) and 3350–3400 cm^{-1} (ν(OH)), probably due to water molecules trapped within the bone´s crystalline framework.

Particularly regarding the carbonate-to-phosphate quantification, the $\nu_3(CO_3^{2-})_B$ band at 1415 cm^{-1} and $\nu_3(CO_3^{2-})_A$ band at 1540 can be severely influenced, respectively, by the methylene deformation modes ($\delta(CH_2)$, at 1420–1460 cm^{-1}) and amide II modes from bone´s organic constituents (lipids and collagen), which have a significant intensity both in intact bone and in samples heated at moderate temperatures [12,21]. This interference was more noteworthy in the CEI/XXI samples, particularly in those subjected to burning at 450 °C.

Bone tissue often displays intrinsic fluorescence [72], mainly arising from the presence of organic components (lipids and proteins) [30]. This complicates Raman acquisition as fluorescence often masks the Raman signals, mainly for samples not subjected to heat or burned at low temperatures. However, Raman spectroscopy is a complementary technique to FTIR that allows to observe vibrational modes that are low IR-absorbers or even not infrared active. In

Table 3
Average (Mean), variation coefficient (VC) and standard error (Std. error) for the infrared spectroscopy ratios and for the Raman carbonate/phosphate index, for the human skeletal samples from the four different sets currently analysed, before and after acetic acid treatment.

	Samples			CEI/XXI 450 °C	CEI/XXI 700 °C	CEI/XXI 800 °C	CEI/XXI 900 °C	ArchR	Arch	Cr
FTIR-ATR	CI	N		24	21	25	23	14	18	24
		Before	Mean	3.29	4.75	3.66	4.14	5.12	4.89	4.96
			VC	4.85	7.42	4.77	7.85	13.12	9.62	14.69
			Std. error	0.16	0.35	0.18	0.33	0.67	0.47	0.73
		After	Mean	3.88	4.92	4.05	5.25	5.43	5.19	5.94
			VC	13.24	7.37	8.75	7.44	10.73	11.15	12.73
			Std. error	0.51	0.36	0.35	0.39	0.58	0.58	0.76
	C/P	N		22	23	25	24	9	15	23
		Before	Mean	.035	0.18	0.21	0.19	0.06	0.16	0.18
			VC	14.49	37.55	15.82	30.64	99.13	55.04	28.85
			Std. error	0.05	0.07	0.03	0.06	0.06	0.09	0.05
		After	Mean	0.20	0.10	0.14	0.07	0.02	0.10	0.23
			VC	44.44	15.81	17.10	25.77	55.50	41.50	81.13
			Std. error	0.09	0.02	0.02	0.02	0.01	0.04	0.19
	API	N		25	20	25	23	12	15	23
		Before	Mean	0.62	0.31	0.34	0.28	0.17	0.18	0.47
			VC	59.48	55.36	33.54	45.02	124.93	118.22	29.04
			Std. error	0.37	0.17	0.12	0.12	0.21	0.22	0.14
		After	Mean	0.40	0.10	0.19	0.07	0.02	0.04	0.10
			VC	93.04	27.92	30.07	29.84	44.83	59.01	59.45
			Std. error	0.38	0.03	0.06	0.02	0.01	0.02	0.06
	BPI	N		25	22	23	22	11	15	22
		Before	Mean	1.64	0.68	1.00	0.67	0.26	0.56	0.73
			VC	13.06	38.41	26.03	40.69	110.05	32.57	24.22
			Std. error	0.21	0.26	0.26	0.27	0.28	0.18	0.18
		After	Mean	0.83	0.36	0.52	0.25	0.05	0.45	0.09
			VC	54.32	41.10	46.82	40.96	80.48	37.57	64.88
			Std. error	0.45	0.15	0.24	0.10	0.4	0.17	0.06
	C/C	N		25	22	23	22	11	15	22
		Before	Mean	1.03	1.05	1.10	0.99	1.73	1.39	1.39
			VC	2.58	4.85	3.46	3.36	19.83	13.16	11.79
			Std. error	0.03	0.05	0.04	0.03	0.34	0.18	0.16
		After	Mean	1.05	1.18	1.14	1.15	2.20	1.58	2.78
			VC	1.91	52.22	5.28	5.43	20.03	8.71	24.70
			Std. error	0.02	0.62	0.06	0.06	0.44	0.14	0.69
	OH/P	N		-	24	25	24	14	18	22
		Before	Mean	-	0.43	0.35	0.43	0.55	0.46	0.57
			VC	-	7.62	12.45	11.40	14.76	12.84	14.16
			Std. error	-	0.03	0.04	0.05	0.08	0.06	0.08
		After	Mean	-	0.41	0.38	0.46	0.54	0.48	0.60
			VC	-	8.38	12.29	5.18	17.24	10.18	12.73
			Std. error	-	0.03	0.38	0.02	0.09	0.05	0.08
Raman	A_{1070}/A_{960}	Before			0.043		0.086	0.032	0.028	0.026
		After			0.040		0.070	0.031	0.030	0.024

particular, it yields very defined and intense bands for the phosphate constituent, which enables evaluating the selectivity of the acetic acid treatment (Table 1). Hence, Raman spectra were also acquired for the samples under study (Fig. 5), allowing to verify that: (i) the area of the $\nu_1(PO_4^{3-})$ band was not affected by acetic acid treatment, with mean values of 14.7, 16.1, 12.7, 14.6, and 11.4 a.u. respectively for samples CEI/XXI/700 °C, CEI/XXI/900 °C, ArchR, Arch and Cr; (ii) the carbonate-to-phosphate ratio – $C/P = A(\nu_1(CO_3^{2-}))/A(\nu_1(PO_4^{3-})) = A_{1070}/A_{960}$ – decreased with acid washing with a more significant effect on present-day bones burned at 900 °C (0.086 and 0.070, respectively before and after treatment).

3.3. Chemometrics

Table 3 comprises the mean values of the most informative infrared and Raman spectroscopic ratios, for each set of human skeletal samples under analysis, before and after acetic acid washing. Fig. 6 depicts the corresponding data of the mean variations and associated ranges. A mean increase of the CI was observed upon acid washing for all types of samples. This was expected since the atomic order in bone decreases for higher carbonate contents [43] which are reduced by the acid treatment. Increased crystallinity was more noteworthy for the present-day cremated bones and the present-day CEI/XXI samples burned at 900 and 450 °C, in agreement with previous reports [24].

Although the Cr and CEI/XXI samples burned at 900 and 450 °C displayed the same behaviour after acetic acid treatment, the characteristics of the three sets of samples were different. Samples burned at 450 °C experienced a large increase in CI, since smaller and more reactive crystals are more easily removed by acetic acid. Consequently, these bones showed a greater margin for recrystallization than the other sets of samples which were already recrystallized or under recrystallization.

Concerning the C/C ratio, all the samples showed an increase after acid treatment, that may be due to a decrease in type-B and type-A carbonates. C/C was found to display a variation in the present-day CEI/XXI bones burned at 450, 700, 800 and 900 °C, in contrast to ArchR or Arch specimens, after acid washing: 1.94%, 13.25%, 3.99% and 15.94% *vs* 27.87 or 15.01% (on average), respectively. Thus, the C/C index appears to has a very large variation between the different CEI/XXI burning temperatures, the 700 and 900 °C values being very similar to those of the ArchR and Arch samples. However, this index has no potential for discrimination between recent and ancient samples. It may, nonetheless, have some potential for discrimination between crematorium samples (C/C=100%) and the remaining samples.

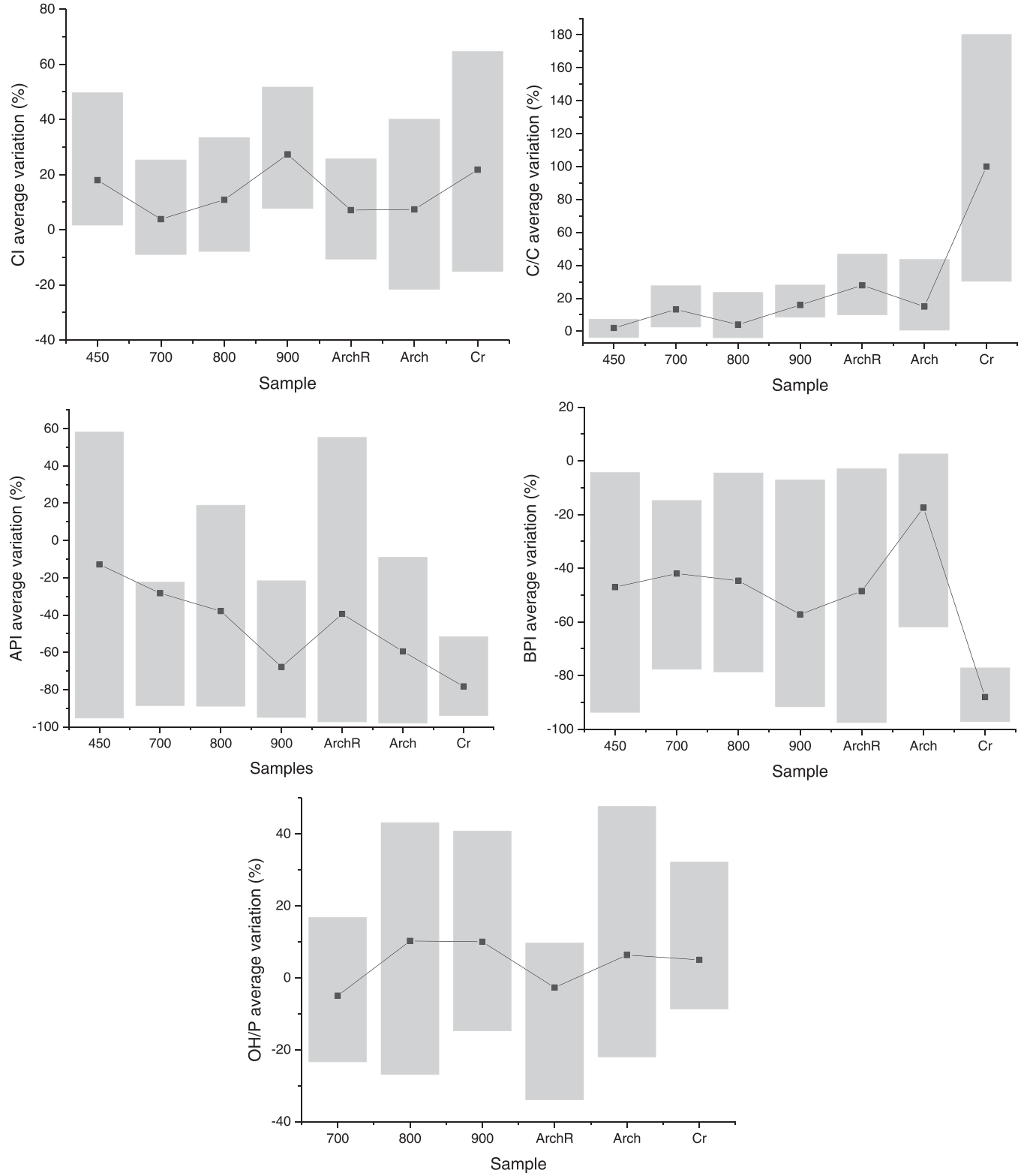

Fig. 6. Mean variation of CI, C/C, API, BPI and OH/P infrared ratios for the human skeletal samples from CEI/XXI (450, 700, 800, 900 °C), ArchR, Arch and Cr, before and after acetic acid treatment. (The variation ranges, in percentage, are represented by the shaded rectangles).

The samples from the crematorium showed an average C/C increase of 100% (variation coefficient (CV of 44.6%), which was even greater than the one observed for archaeological bones. This increase was caused by high losses of carbonates A (API=−78.31%) and carbonates B (BPI=−88.02%). The crematorium samples were heavily enriched with carbonates most probably due to the presence of wood (coffin) and methane during cremation. Methane was the fuel used in the cremation process which ignited, when in contact with oxygen from the furnace environment, the release of CO_2 subsequently absorbed by the bone surface. As modern cremation was performed within a closed environment, Cr samples thus acquired large amounts of carbonates. This hypothesis is in agreement with

Table 4
Summary of the main conclusions obtained in the present study regarding acetic acid treatment of burned skeletal samples.

Samples	Main conclusions
CEI/XXI 450 °C	✓ Smallest carbonates reduction ✓ Significant increase of CI
CEI/XXI 900 °C	✓ Most significant decrease of C/P (Raman) ✓ Most substantial increase of CI ✓ Significant decrease of API ✓ Significant decrease of BPI
ArchR Arch Cr	✓ Largest carbonate reduction ✓ Detection of portlandite ($Ca(OH)_2$) ✓ Second largest increase of CI ✓ Largest increase of C/C ✓ Largest decrease of API ✓ Largest decrease of BPI ✓ Detection of portlandite ($Ca(OH)_2$) ✓ Detection of exogenous carbonates (mostly due to contamination from methane during cremation)

Snoeck et al., who also observed that fuel and wood contribute greatly to the carbonate content of bone samples [73]. This fact can justify the failure of the acetic acid treatment to completely remove the carbonates from these types of cremated samples, the bands at 1412, 1459 and 1549 cm^{-1} (assigned to carbonates) being still detected in the corresponding FTIR spectrum (Fig. 4).

Regarding the API ratio, a mean carbonate reduction was observed for all sets of bones under analysis. Such reduction was larger for present-day CEI/XXI samples burned at 900 °C and present-day cremated bone samples, that displayed API values of − 67.86% (CV=27,5%) and − 78.31% (CV=15,39%), respectively. However, a significant increase in carbonates was verified for a few ArchR and CEI/XXI samples (burned at 450 and 800 °C). Hypothetically, such an increase (in carbonates A) may reflect a transfer of carbonates B to carbonate A sites. In addition, the BPI index decreased for all samples mainly for present-day CEI/XXI/900 °C specimens and for present-day cremated bones, with values equal to − 57.22% (CV=36.96%) and − 88.02% (CV=7.29%), respectively. Therefore, the data presently gathered evidence a more significant loss of carbonates B relative to carbonates A. This was to be expected since type B carbonate substitutions are more common than type A. Hence, both B to A carbonate transfer and the pronounced loss of B-type carbonates justify the observed increase of the C/C ratio.

The most pronounced carbonate losses in recent samples had already been reported by Snoeck et al. and may be due to the lower crystallinity of modern specimens, containing smaller crystallites more easily accessed by the acid [24]. Additionally, former studies have reported that present-day bones, still very reactive and undergoing early diagenetic processes, appear to be more sensitive to chemical treatment as opposed to older and less reactive bones [37]. The removal of the carbonates from the bone matrix in an aqueous medium is associated with the recrystallization process of bioapatite during which the re-entrance of OH^- anions into its framework, to occupy the places left by the carbonates (Table 3, Fig. 4).

The cremated bones (Cr) constitute a very specific type of skeletal remains, with a high crystallinity (the highest CI value presently measured, 5.94, Table 3, Fig. 4) and a very low concentration of exogenous trace elements. High CI values have already been obtained by the authors for recent burned bones at high temperature [12]. These samples displayed a distinctive infrared profile when compared to the other three sets of bones, particularly regarding the bands at 3640 cm^{-1} (ascribed to portlandite, $Ca(OH)_2$) and three well defined features at 1413, 1459 and 1549 cm^{-1} that are assigned to traces of carbonates (type B, A+B and A, respectively) and remain after acid treatment (as opposed to ArchR for which this pattern disappears upon acetic acid washing). They were found to be significantly affected by acid treatment, although their chemical and structural properties have already been drastically altered by the very intense burning (at *ca.* 1000 – 1100 °C) during the cremation process, as previously observed in medieval cremated human bones [37]. Additionally, these samples can be taken as a reference relative to archaeological and modern bones, as they are completely devoid of organic constituents and display the highest degree of structural order (provided there is no significant contamination during cremation) [37]. Moreover, the influence of soft tissues during the burning process must be taken into account, as well as the high amount of carbon dioxide formed during aerobic cremation (in an oven fed by methane gas such as the one used in the Trieste crematorium which was the source of the present samples). Both these factors are prone to significantly increase the amount of carbonate adsorbed by the bones. In addition, the cadavers were cremated with their clothes on, inside a wooden coffin – so interferences from the cloth materials and pigments, as well as from the wood, should not be disregarded. In turn, the CEI/XXI and ArchR samples presently analysed were defleshed bones, while the Arch bones were probably burned with soft tissues but in open air settings (*e.g.* wooden pyre cremations). The extremely high carbonate content in the Cr samples was evidenced by the variation of the API and C/P ratios upon acid treatment, which is larger than for all other samples (Table 3, Fig. 4).

The chemical treatment of bones with acetic acid was highly selective – while it prompted a marked carbonate decrease, the remaining inorganic matrix (calcium phosphate and hydroxyl groups) was left virtually unaffected. This was evidenced by: (i) the FTIR-ATR spectra, which displayed no considerable variations of the hydroxyapatite bands, before and after acid washing (Fig. 4); (ii) the Raman data, showing unchanged phosphate bands even upon acid treatment (Fig. 5); and (iii) the infrared OH/P index, which remained almost constant before and after chemical handling (Fig. 6).

The Raman spectral profiles obtained for the distinct bones under study also evidenced a higher crystallinity of the CEI/XXI and Cr samples (particularly for the latter), which displayed a remarkable similarity to the spectra of reference hydroxyapatite (Fig. 5). Moreover, analysis of the areas of the Raman signals at 1073 and 960 cm^{-1} assigned to carbonate ($\nu_1(CO_3^{2-})$,) and phosphate ($\nu_1(PO_4^{3-})$), respectively, allowed to corroborate the infrared results: (i) the area of the $\nu_1(PO_4^{3-})$ band remains virtually unaffected by acid treatment, for the CEI/XXI, ArchR, Arch and Cr sets of samples; (ii) the carbonate-to-phosphate ratio decreases upon acid washing, this effect being more noteworthy for the recent bones burned at 900 °C (0.086 *vs* 0.070, respectively before and after acid treatment). In addition, no broadening of the phosphate vibrational bands (either infrared or Raman) was observed upon acetic acid treatment for any of the bone groups under analysis, which evidences a specific impact of the acid on bone´s carbonate components (intrinsic, types A and B, and extrinsic), leaving the phosphates unaltered (*i.e.,* there is no dissolution of hydroxyapatite).

4. Conclusions

Overall, it may be concluded that acetic acid washing of skeletal remains, currently assessed by infrared and Raman spectroscopies, is an effective method for carbonate removal (both exogenous and endogenous carbonates), as well as possible contaminants such as calcium hydroxide. This effect was found to depend on the type of bone, regarding its source, age and burning process (Table 4). Furthermore, this chemical process was shown to be highly specific, leaving the phosphate matrix virtually unaffected (as evidenced by both infrared and Raman).

Despite the distinct impact of the acid treatment on the different types of bones, it proved to be insufficient for an unequivocal discrimination between present-day and archaeological bones. Nevertheless, the C/C spectroscopic index was identified as a

possible indicator for recognising present-day bones burned in a gas-fuelled crematorium from other skeletal remains (either ancient or modern) burned under distinct conditions. Regrettably, such potential is of little use because the need to differentiate present-day cremated from other types of burned bones is not usually raised.

CRediT authorship contribution statement

A.L. Brandão – Experimental procedures (sample preparation, acetic acid treatment, FTIR and Raman measurements) and manuscript writing. **L.A.E. Batista de Carvalho** – conceptualization, FTIR and Raman measurements, data analysis and revising manuscript. **D. Gonçalves** – conceptualization, data analysis and manuscript writing. **G. Piga** – provision of bone samples (Trieste crematorium and *El Inchidero* necropolis) and revising manuscript; **E. Cunha** – provision of bone samples (CEI/XXI collection) and revising manuscript. **M.P.M. Marques** – conceptualization, data analysis, and manuscript writing. All authors have read and agreed to the published version of the manuscript.

Data Availability

The data that support the findings of this study are available from the corresponding author upon reasonable request.

Declaration of Competing Interest

The authors have no competing interests to declare.

Acknowledgments

The authors acknowledge financial support from the Portuguese Foundation for Science and Technology (UIDB/00070/2020; UIDP/00070/2020). We are grateful do Dr. Ana Maria Silva for providing archaeological bone samples from the *Hospital Real de Santo António*. The authors also thank Dr. Fabio Cavalli [Research Unit of Paleoradiology and Allied Sciences, Julian-Isontine Universitary Integrated Health Enterprise (ASUGI), Trieste-Italy for supplying the (II) set of bones samples employed in this study.

Novelty statement

This is an original study on the application of an acetic acid treatment to bone, aiming at removing contaminants and carbonates in order to assist discrimination between ancient and present-day skeletal remains through infrared spectroscopic analysis.

Supplementary information

The Supplementary Information contains Fig. S1 - FTIR-ATR spectra (400 – 4000 cm^{-1}) of porcine femur, before and after acetic acid treatment with acetic acid 0.1 M for 4 h and Table S1 – Human skeleton samples (present-day and archaeological) analysed in the present study. (The burning temperatures and times are also included).

Appendix A. Supporting information

Supplementary data associated with this article can be found in the online version at doi:10.1016/j.forsciint.2023.111690.

References

[1] L.A. Currie, The remarkable metrological history of radiocarbon dating [II], J. Res. Natl. Inst. Stand. Technol. 109 (2004) 185–217, https://doi.org/10.6028/JRES.109.013

[2] F. Introna, G. Di Vella, C.P. Campobasso, Determination of postmortem interval from old skeletal remains by image analysis of luminol test results, J. Forensic Sci. 44 (1999) 14505J, https://doi.org/10.1520/jfs14505j

[3] C. Ermida, D. Navega, E. Cunha, Luminol chemiluminescence: contribution to postmortem interval determination of skeletonized remains in Portuguese forensic context, Int. J. Leg. Med. 131 (2017) 1149–1153, https://doi.org/10.1007/s00414-017-1547-0

[4] H.P. Schwarcz, K. Agur, L.M. Jantz, A new method for determination of postmortem interval: Citrate content of bone, J. Forensic Sci. 55 (2010) 1516–1522, https://doi.org/10.1111/j.1556-4029.2010.01511.x

[5] S.J. Wilson, A.M. Christensen, A test of the citrate method of PMI estimation from skeletal remains, Forensic Sci. Int. 270 (2017) 70–75, https://doi.org/10.1016/j.forsciint.2016.11.026

[6] C.N. Trueman, K. Privat, J. Field, Why do crystallinity values fail to predict the extent of diagenetic alteration of bone mineral? Palaeogeogr. Palaeoclimatol. Palaeoecol. 266 (2008) 160–167, https://doi.org/10.1016/j.palaeo.2008.03.038

[7] T.J.U. Thompson, M. Gauthier, M. Islam, The application of a new method of Fourier Transform Infrared Spectroscopy to the analysis of burned bone, J. Archaeol. Sci. 36 (2009) 910–914, https://doi.org/10.1016/j.jas.2008.11.013

[8] M.M. Cascant, S. Rubio, G. Gallello, A. Pastor, S. Garrigues, M. de la Guardia, Burned bones forensic investigations employing near infrared spectroscopy, Vib. Spectrosc. 90 (2017) 21–30, https://doi.org/10.1016/j.vibspec.2017.02.005

[9] M.P.M. Marques, A.P. Mamede, A.R. Vassalo, C. Makhoul, E. Cunha, D. Gonçalves, S.F. Parker, L.A.E. Batista de Carvalho, Heat-induced bone diagenesis probed by vibrational spectroscopy, Sci. Rep. 8 (2018) Art. 15935, https://doi.org/10.1038/s41598-018-34376-w

[10] A.P. Mamede, A.R. Vassalo, G. Piga, E. Cunha, S.F. Parker, M.P.M. Marques, L.A.E. Batista de Carvalho, D. Gonçalves, Potential of bioapatite hydroxyls for research on archeological burned bone, Anal. Chem. 90 (2018) 11556–11563, https://doi.org/10.1021/acs.analchem.8b02868

[11] A.P. Mamede, D. Gonçalves, M.P.M. Marques, L.A.E. Batista de Carvalho, Burned bones tell their own stories: A review of methodological approaches to assess heat-induced diagenesis, Appl. Spectrosc. Rev. 53 (2018) 603–635, https://doi.org/10.1080/05704928.2017.1400442

[12] D. Gonçalves, A.R. Vassalo, A.P. Mamede, C. Makhoul, G. Piga, E. Cunha, M.P.M. Marques, L.A.E. Batista de Carvalho, Crystal clear: Vibrational spectroscopy reveals intrabone, intraskeleton, and interskeleton variation in human bones, Am. J. Phys. Anthr. 166 (2018) 296–312, https://doi.org/10.1002/ajpa.23430

[13] G.F. Monnier, A review of infrared spectroscopy in microarchaeology: Methods, applications, and recent trends, J. Archaeol. Sci. Rep. 18 (2018) 806–823, https://doi.org/10.1016/j.jasrep.2017.12.029

[14] T. Leskovar, I. Zupanič Pajnič, I. Jerman, M. Črešnar, Separating forensic, WWII, and archaeological human skeletal remains using ATR-FTIR spectra, Int. J. Leg. Med. (2019), https://doi.org/10.1007/s00414-019-02079-0

[15] A. van Hoesel, F.H. Reidsma, B.J.H. van Os, L. Megens, F. Braadbaart, Combusted bone: Physical and chemical changes of bone during laboratory simulated heating under oxidising conditions and their relevance for the study of ancient fire use, J. Archaeol. Sci. Rep. 28 (2019) 102033, https://doi.org/10.1016/j.jasrep.2019.102033

[16] G. Festa, C. Andreani, M. Baldoni, V. Cipollari, C. Martínez-Labarga, F. Martini, O. Rickards, M.F. Rolfo, L. Sarti, N. Volante, R. Senesi, F.R. Stasolla, S.F. Parker, A.R. Vassalo, A.P. Mamede, L.A.E. Batista de Carvalho, M.P.M. Marques, First analysis of ancient burned human skeletal remains probed by neutron and optical vibrational spectroscopy, Sci. Adv. 5 (2019) eaaw1292, https://doi.org/10.1126/sciadv.aaw1292

[17] D. Gonçalves, A.R. Vassalo, C. Makhoul, G. Piga, A.P. Mamede, S.F. Parker, M.T. Ferreira, E. Cunha, M.P.M. Marques, L.A.E. Batista de Carvalho, Chemosteometric regression models of heat exposed human bones to determine their pre-burnt metric dimensions, Am. J. Phys. Anthropol. 173 (2020) 734–747, https://doi.org/10.1002/ajpa.24104

[18] D. Roche, L. Ségalen, E. Balan, S. Delattre, Preservation assessment of Miocene-Pliocene tooth enamel from Tugen Hills (Kenyan Rift Valley) through FTIR, chemical and stable-isotope analyses, J. Archaeol. Sci. 37 (2010) 1690–1699, https://doi.org/10.1016/j.jas.2010.01.029

[19] G. Festa, G. Romanelli, R. Senesi, L. Arcidiacono, C. Scatigno, S.F. Parker, M.P.M. Marques, C. Andreani, Neutrons for cultural heritage—techniques, sensors, and detection, Sensors 20 (2020) 502, https://doi.org/10.3390/s20020502

[20] M.P.M. Marques, D. Gonçalves, A.P. Mamede, T. Coutinho, E. Cunha, W. Kockelmann, S.F. Parker, L.A.E. Batista de Carvalho, Profiling of human burned bones: oxidising versus reducing conditions, Sci. Rep. 11 (2021) Art. 1361, https://doi.org/10.1038/s41598-020-80462-3

[21] M.P.M. Marques, L.A.E. Batista de Carvalho, D. Gonçalves, E. Cunha, S.F. Parker, The impact of moderate heating on human bones: An infrared and neutron spectroscopy study, R. Soc. Open Sci. (2021) 210774, https://doi.org/10.1098/rsos.210774

[22] T.J.U. Thompson, M. Islam, M. Bonniere, A new statistical approach for determining the crystallinity of heat-altered bone mineral from FTIR spectra, J. Archaeol. Sci. 40 (2013) 416–422, https://doi.org/10.1016/j.jas.2012.07.008

[23] H.I. Hollund, F. Ariese, R. Fernandes, M.M.E. Jans, H. Kars, Testing an alternative high-throughput tool for investigating bone diagenesis: Ftir in attenuated total reflection (atr) mode, Archaeometry 55 (2013) 507–532, https://doi.org/10.1111/j.1475-4754.2012.00695.x

[24] C. Snoeck, J.A. Lee-Thorp, R.J. Schulting, From bone to ash: Compositional and structural changes in burned modern and archaeological bone, Palaeogeogr.

Palaeoclimatol. Palaeoecol. 416 (2014) 55–68, https://doi.org/10.1016/j.palaeo.2014.08.002
[25] M. Lebon, A. Zazzo, I. Reiche, Screening in situ bone and teeth preservation by ATR-FTIR mapping, Palaeogeogr. Palaeoclimatol, Palaeoecol 416 (2014) 110–119, https://doi.org/10.1016/j.palaeo.2014.08.001
[26] A. Grunenwald, C. Keyser, A.M. Sautereau, E. Crubezy, B. Ludes, C. Drouet, Revisiting carbonate quantification in apatite (bio)minerals: a validated FTIR methodology, J. Archaeol. Sci. 49 (2014) 134–141, https://doi.org/10.1016/j.jas.2014.05.004
[27] M.P.M. Marques, D. Gonçalves, A.I.C. Amarante, C.I. Makhoul, S.F. Parker, L.A.E. Batista de Carvalho, Osteometrics in burned human skeletal remains by neutron and optical vibrational spectroscopy, RSC Adv. 6 (2016) 68638–68641, https://doi.org/10.1039/c6ra13564a
[28] G. Piga, M.D. Baró, I.G. Escobal, D. Gonçalves, C. Makhoul, A. Amarante, A. Malgosa, S. Enzo, S. Garroni, A structural approach in the study of bones: fossil and burnt bones at nanosize scale, Appl. Phys. A Mater. Sci. Process. 122 (2016) 1–12, https://doi.org/10.1007/s00339-016-0562-1
[29] G. Piga, D. Gonçalves, T.J.U. Thompson, A. Brunetti, A. Malgosa, S. Enzo, Understanding the crystallinity indices behavior of burned bones and teeth by ATR-IR and XRD in the presence of bioapatite mixed with other phosphate and carbonate phases, Int. J. Spectrosc. 2016 (2016) 1–9, https://doi.org/10.1155/2016/4810149
[30] F.H. Reidsma, A. van Hoesel, B.J.H. van Os, L. Megens, F. Braadbaart, Charred bone: physical and chemical changes during laboratory simulated heating under reducing conditions and its relevance for the study of fire use in archaeology, J. Archaeol. Sci. Rep. 10 (2016) 282–292, https://doi.org/10.1016/j.jasrep.2016.10.001
[31] G. Abdel-Maksoud, A. El-Sayed, Analysis of archaeological bones from different sites in Egypt by a multiple techniques (XRD, EDX, FTIR), Mediterr, Archaeol. Archaeom. 16 (2016) 149–158, https://doi.org/10.5281/zenodo.53073
[32] J.I. Lachowicz, S. Palomba, P. Meloni, M. Carboni, G. Sanna, R. Floris, V. Pusceddu, M. Sarigu, Multi analytical technique study of human bones from an archaeological discovery, J. Trace Elem. Med. Biol. 40 (2017) 54–60, https://doi.org/10.1016/j.jtemb.2016.12.006
[33] A.P. Mamede, A.R. Vassalo, E. Cunha, D. Gonçalves, S.F. Parker, L.A.E. Batista de Carvalho, M.P.M. Marques, Biomaterials from human bone-probing organic fraction removal by chemical and enzymatic methods, RSC Adv. 8 (2018) 27260–27267, https://doi.org/10.1039/c8ra05660a
[34] J.M. Howes, B.H. Stuart, P.S. Thomas, S. Raja, C. O'Brien, An investigation of model forensic bone in soil environments studied using infrared spectroscopy, J. Forensic Sci. 57 (2012) 1161–1167, https://doi.org/10.1111/j.1556-4029.2012.02236.x
[35] Q. Wang, Y. Zhang, H. Lin, S. Zha, R. Fang, X. Wei, S. Fan, Z. Wang, Estimation of the late postmortem interval using FTIR spectroscopy and chemometrics in human skeletal remains, Forensic Sci. Int. 281 (2017) 113–120, https://doi.org/10.1016/j.forsciint.2017.10.033
[36] C. Woess, S.H. Unterberger, C. Roider, M. Ritsch-Marte, N. Pemberger, J. Cemper-Kiesslich, P. Hatzer-Grubwieser, W. Parson, J.D. Pallua, Assessing various Infrared (IR) microscopic imaging techniques for post-mortem interval evaluation of human skeletal remains, PLoS One 12 (2017) 1–16, https://doi.org/10.1371/journal.pone.0174552
[37] R. McMillan, C. Snoeck, N.J. de Winter, P. Claeys, D. Weis, Evaluating the impact of acetic acid chemical pre-treatment on 'old' and cremated bone with the 'Perio-spot' technique and 'Perios-endos' profiles, Palaeogeogr. Palaeoclimatol. Palaeoecol. 530 (2019) 330–344, https://doi.org/10.1016/j.palaeo.2019.05.019
[38] T. Leskovar, I. Zupanič Pajnič, I. Jerman, M. Črešnar, Preservation state assessment and post-mortem interval estimation of human skeletal remains using ATR-FTIR spectra, Aust. J. Forensic Sci. 00 (2020) 1–22, https://doi.org/10.1080/00450618.2020.1836254
[39] B. Wopenka, J.D. Pasteris, A mineralogical perspective on the apatite in bone, Mater. Sci. Eng. C. 25 (2005) 131–143, https://doi.org/10.1016/j.msec.2005.01.008
[40] C. Rey, C. Combes, C. Drouet, M.J. Glimcher, Bone mineral: update on chemical composition and structure, Natl, Inst. Heal 20 (2010) 1013–1021, https://doi.org/10.1007/s00198-009-0860-y.Bone
[41] X.Y. Wang, Y. Zuo, D. Huang, X.D. Hou, Y.B. Li, Comparative study on inorganic composition and crystallographic properties of cortical and cancellous bone, Biomed. Environ. Sci. 23 (2010) 473–480, https://doi.org/10.1016/S0895-3988(11)60010-X
[42] H. Madupalli, B. Pavan, M.M.J. Tecklenburg, Carbonate substitution in the mineral component of bone: Discriminating the structural changes, simultaneously imposed by carbonate in A and B sites of apatite, J. Solid State Chem. 255 (2017) 27–35, https://doi.org/10.1016/j.jssc.2017.07.025
[43] A. Deymier, A. Nair, B. Depalle, Q. Zhao, K. Arcot, C. Drouet, C. Yoder, M. Buehler, S. Thomopoulos, G. Genin, J.D. Pasteris, Protein-free formation of bone-like apatite: New insights into the key role of carbonation, Biomaterials 127 (2017) 75–88, https://doi.org/10.1016/j.biomaterials.2017.02.029.
[44] D.H. Ubelaker, The forensic evaluation of burned skeletal remains: A synthesis, Forensic Sci. Int. 183 (2009) 1–5, https://doi.org/10.1016/j.forsciint.2008.09.019
[45] S.T.D. Ellingham, T.J.U. Thompson, M. Islam, G. Taylor, Estimating temperature exposure of burnt bone - A methodological review, Sci. Justice 55 (2015) 181–188, https://doi.org/10.1016/j.scijus.2014.12.002
[46] G. Festa, A.P. Mamede, D. Gonçalves, E. Cunha, W. Kockelmann, S.F. Parker, L.A.E. Batista de Carvalho, M.P.M. Marques, In-situ anaerobic heating of human bones probed by neutron diffraction, Anal. Chem. 95 (2023) 2469–2477, https://doi.org/10.1021/acs.analchem.2c04721
[47] S.D. Emslie, R. Brasso, W.P. Patterson, A. Carlos Valera, A. McKenzie, A. Maria Silva, J.D. Gleason, J.D. Blum, Chronic mercury exposure in Late Neolithic/Chalcolithic populations in Portugal from the cultural use of cinnabar, Sci. Rep. 5 (2015) 1–9, https://doi.org/10.1038/srep14679
[48] L.E. Wright, H.P. Schwarcz, Infrared and isotopic evidence for diagenesis of bone apatite at Dos Pilas, Guatemala: Palaeodietary implications, J. Archaeol. Sci. 23 (1996) 933–944, https://doi.org/10.1006/jasc.1996.0087
[49] C.M. Nielsen-Marsh, R.E.M. Hedges, Patterns of diagenesis in bone II: Effects of acetic acid treatment and the removal of diagenetic CO32, J. Archaeol. Sci. 27 (2000) 1151–1159, https://doi.org/10.1006/jasc.1999.0538
[50] S.J. Garvie-Lok, T.L. Varney, M.A. Katzenberg, Preparation of bone carbonate for stable isotope analysis: The effects of treatment time and acid concentration, J. Archaeol. Sci. 31 (2004) 763–776, https://doi.org/10.1016/j.jas.2003.10.014
[51] A. Zazzo, M. Lebon, L. Chiotti, C. Comby, E.D.Ë. Roland, N. Ina, Can we use calcined boes for 14C Dating the paleolithic? Radiocarbon 55 (2013) 1409–1421, https://hal.science/hal-02351835.
[52] C.J. Yoder, E.J. Bartelink, Effects of different sample preparation methods on stable carbon and oxygen isotope values of bone apatite: A comparison of two treatment protocols, Archaeometry 52 (2010) 115–130, https://doi.org/10.1111/j.1475-4754.2009.00473.x
[53] J. Hellawell, C.J. Nicholas, Acid treatment effects on the stable isotopic signatures of fossils, Palaeontology 55 (2012) 1–10, https://doi.org/10.1111/j.1475-4983.2011.01108.x
[54] M.M. Beasley, E.J. Bartelink, L. Taylor, R.M. Miller, Comparison of transmission FTIR, ATR, and DRIFT spectra: Implications for assessment of bone bioapatite diagenesis, J. Archaeol. Sci. 46 (2014) 16–22, https://doi.org/10.1016/j.jas.2014.03.008
[55] C. Snoeck, J. Pouncett, P. Claeys, S. Goderis, N. Mattielli, M. Parker Pearson, C. Willis, A. Zazzo, J.A. Lee-Thorp, R.J. Schulting, Strontium isotope analysis on cremated human remains from Stonehenge support links with west Wales, Sci. Rep. 8 (2018) 1–8, https://doi.org/10.1038/s41598-018-28969-8
[56] J.A. Lee-Thorp, N.J. van der Merwe, Aspects of the chemistry of modern and fossil biological apatites, J. Archaeol. Sci. 18 (1991) 343–354, https://doi.org/10.1016/0305-4403(91)90070-6
[57] P.L. Koch, N. Tuross, M.L. Fogel, The effects of sample treatment and diagenesis on the isotopic integrity of carbonate in biogenic hydroxylapatite, J. Archaeol. Sci. 24 (1997) 417–429, https://doi.org/10.1006/jasc.1996.0126
[58] M.T. Ferreira, C. Coelho, C. Makhoul, D. Navega, D. Gonçalves, E. Cunha, F. Curate, New data about the 21st Century Identified Skeletal Collection (University of Coimbra, Portugal), Int. J. Leg. Med. 135 (2021) 1087–1094, https://doi.org/10.1007/s00414-020-02399-6
[59] A.R. Vassalo, E. Cunha, L.A.E. Batista de Carvalho, D. Gonçalves, Rather yield than break: assessing the influence of human bone collagen content on heat-induced warping through vibrational spectroscopy, Int. J. Leg. Med. 130 (2016) 1647–1656, https://doi.org/10.1007/s00414-016-1400-x
[60] A. Mamede, Burned Bones: A Comparation of Methodological Approaches to Assess Heat-induced Alterations, MSc thesis, University of Coimbra, 2017, https://estudogeral.uc.pt/handle/10316/82888.
[61] S. Weiner, O. Bar-Yosef, States of preservation of bones from prehistoric sites in the Near East: A survey, J. Archaeol. Sci. 17 (1990) 187–196, https://doi.org/10.1016/0305-4403(90)90058-D
[62] A.M.C. Baptista, Estimativa do Intervalo Postmortem a Partir da Composição Química Óssea Analisada por FTIR-ATR, Master thesis, Univ. Coimbra (2020), https://estudogeral.uc.pt/handle/10316/92252.
[63] A. Roschger, S. Gamsjaeger, B. Hofstetter, A. Masic, S. Blouin, P. Messmer, A. Berzlanovich, E.P. Paschalis, P. Roschger, K. Klaushofer, P. Fratzl, Relationship between the v2PO4/amide III ratio assessed by Raman spectroscopy and the calcium content measured by quantitative backscattered electron microscopy in healthy human osteonal bone, J. Biomed. Opt. 19 (2014) 065002, https://doi.org/10.1117/1.jbo.19.6.065002
[64] M. Sponheimer, J.A. Lee-Thorp, Alteration of enamel carbonate environments during fossilization, J. Archaeol. Sci. 26 (1999) 143–150, https://doi.org/10.1006/jasc.1998.0293
[65] C. Rey, B. Collins, T. Goehl, I.R. Dickson, M.J. Glimcher, The carbonate environment in bone mineral: A resolution-enhanced fourier transform infrared spectroscopy study, Calcif. Tissue Int. 45 (1989) 157–164, https://doi.org/10.1007/BF02556059
[66] N. Keough, E.N. L'Abbé, M. Steyn, S. Pretorius, Assessment of skeletal changes after post-mortem exposure to fire as an indicator of decomposition stage, Forensic Sci. Int. 246 (2015) 17–24, https://doi.org/10.1016/j.forsciint.2014.10.042
[67] B.S. Hudson, Inelastic neutron scattering: a tool in molecular vibrational spectroscopy and a test of ab initio methods, J. Phys. Chem. A. 105 (2001) 3949–3960, https://doi.org/10.1021/jp004429o
[68] D. Farlay, G. Panczer, C. Rey, P.D. Delmas, G. Boivin, Mineral maturity and crystallinity index are distinct characteristics of bone mineral, J. Bone Miner. Metab. 28 (2010) 433–445, https://doi.org/10.1007/s00774-009-0146-7
[69] M. Lebon, K. Müller, J.J. Bahain, F. Fröhlich, C. Falguères, L. Bertrand, C. Sandt, I. Reiche, Imaging fossil bone alterations at the microscale by SR-FTIR

microspectroscopy, J. Anal. Spectrom. 26 (2011) 922–929, https://doi.org/10.1039/c0ja00250j
[70] B.S. Hudson, Vibrational spectroscopy using inelastic neutron scattering: Overview and outlook, Vib. Spectrosc. 42 (2006) 25–32, https://doi.org/10.1016/j.vibspec.2006.04.014
[71] C.N.G. Trueman, A.K. Behrensmeyer, N. Tuross, S. Weiner, Mineralogical and compositional changes in bones exposed on soil surfaces in Amboseli National Park, Kenya: Diagenetic mechanisms and the role of sediment pore fluids, J. Archaeol. Sci. 31 (2004) 721–739, https://doi.org/10.1016/j.jas.2003.11.003
[72] C.H. Bachman, E.H. Ellis, Fluorescence of Bone, Nat. Publ. Gr. 205 (1965) 498–499.
[73] C. Snoeck, F. Brock, R.J. Schulting, Carbon exchanges between bone apatite and fuels during cremation: impact on radiocarbon dates, Radiocarbon 56 (2014) 591–602, https://doi.org/10.2458/56.17454